BMC Genomics

RESEARCH

Open Access

Functions of thyroid hormone signaling in regulating melanophore, iridophore, erythrophore, and pigment pattern formation in spotted scat (*Scatophagus argus*)

Yongguan Liao[1], Tong Han[1], Dongneng Jiang[1], Chunhua Zhu[1,2], Gang Shi[1], GuangLi Li[1] and Hongjuan Shi[1*]

Abstract

Background Spotted scat, a marine aquaculture fish, has variable body color development stages during their ontogenesis. However, the regulatory mechanism of body color patterns formation was poorly understood. Thyroid hormones (TH) function as an important endocrine factor in regulating metamorphosis. In this study, exogenous thyroid hormones 3,5,3'-L-triiodothyronine (T3) and its inhibitor thiourea (TU) were used to treat spotted scat juveniles during the metamorphosis stage (from 60 to 90 dpf). The function and molecular mechanism of thyroid hormone signaling in regulating body color patterns formation was revealed, using the micro-observation of pigments cells distribution, colorimetric evaluation and carotenoids concentration measurement by spectrophotometry, and comparative transcriptome analysis.

Results Spotted scat body color patterns consisted of whole body black color, black bar, black and red spots, and its final pattern was formed through the metamorphosis. When spotted scat were treated with the inhibitor TU to disrupt thyroid hormone signaling, the levels of T3 and T4 were significantly decreased, the melanophores numbers were significantly increased, as well as the expression of genes involved in melanin synthesis and melanophore differentiation (*tyr*, *tyrp1*, *dct*, *mitf*, *pmel*, *oca2*, *slc24a5*, and *erbb3*) was significantly increased. Besides, the expression of genes associated with carotenoids and pteridine metabolism (*apod*, *pnpla2*, *rdh12*, *stard10*, *xdh*, *abca1*, *retsat*, *scarb1*, *rgs2*, and *gch1*) and carotenoids accumulation were stimulated, when thyroid hormone signaling was disrupted by TU. On the contrary, the levels of T3 and T4 were significantly elevated in spotted scat treated with T3, which could weaken the skin redness and reduce the number of black spots and melanophores, as well as the number and diameter of larval erythrophores. Notably, unlike melanophores and erythrophores, the differentiation of iridophore was promoted by thyroid hormones, gene related to iridophore differentiation (*fhl2-l*, *fhl2*, *ltk*, *id2a*, *alx4*) and guanine metabolism (*gmps*, *hprt1*, *ppat*, *impdh1b*) were up-regulated after T3 treatment, but they were down-regulated after TU treatment.

Conclusions Above results showed that thyroid hormone signaling might play critical roles in regulation pigments synthesis and deposition, thereby affecting pigment cells (melanophores, iridophores and erythrophores) formation and body color patterns. The mechanisms of hyperthyroid and hypothyroid on different pigment cells development were different. Excess thyroid hormone might impact the rearrangement of melanophore by regulating cell cycle, resulting in the abnormalities of black spots in spotted scat. Meanwhile, the excessed thyroid hormone could reduce

*Correspondence:
Hongjuan Shi
shihj@gdou.edu.cn
Full list of author information is available at the end of the article

the number and diameter of larval erythrophores, as well as weaken the skin redness of juvenile erythrophores, but they were enhanced by the disruption of thyroid hormone. However, the formation of iridophore differentiation and guanine synthesis genes expression were stimulated by thyroid hormones. These findings provide new insights for exploring the formation of body color patterns in fish, and help to elucidate the molecular mechanism of thyroid hormone in regulating pigment cell development and body coloration, and may also contribute to selective breeding of ornamental fish.

Keywords Spotted scat, Thyroid hormones, Erythrophore, Pigment pattern, Gene expression

Background

Among vertebrates, teleosts exhibit diverse body color patterns and pigment cells. It is widely recognized that the formation of body color patterns in fish is the result of intricate interactions among different pigment cells, nervous system, and endocrine system [1–5]. The arrangement, overlap, and interaction of different pigment cells culminate in the formation of body color patterns, such as stripes, spots, and bars [1–3]. In fish, several distinct types of pigment cells, varying in chemical composition and reflectance properties, have been identified, including melanophores (black-brown), iridophores (metallic iridescence, silver and white), leucophores (shiny white-yellow), xanthophores (yellow-orange), erythrophores (red) [6]. Melanin formation has been well identified and elucidated, and a large number of associated genes and signaling pathways are revealed, including Wnt signaling pathway, MAPK signaling pathway, melanocortin system, and tyrosinase gene family [7]. The tyrosinase gene family members, such as tyrosinase (*tyr*), tyrosinase-related protein 1 (*tyrp1*) and dopachrome tautomerase (*dct*) have been proved to be crucial for the catalysis and synthesis of melanin, and melanophore formation [8]. Furthermore, the expression of these genes was regulated by the microphthalamia-associated transcription factor (*mift*) [9]. Premelanosome protein (*pmel*) and oculocutaneous albinism II (*oca2*) are critical for the melanosomes survival, their mutations could cause the albinism [10–13]. Erythrophores and xanthophores are the closely related pigment cells that share a common progenitor in *Danio albolineatus* [14]. Some factors related to carotenoids metabolism and erythrophore coloration have been identified, such as StAR related lipid transfer domain containing 10 (*stard10*), apolipoprotein D (*apod*), patatin like phospholipase domain containing 2 (*pnpla2*), retinol dehydrogenase 12 (*rdh12*), and scavenger receptor class B member 1 (*scarb1*) [15]. Disruption of *scarb1* using CRISPR/Cas9, the red skin was faded into white color in Oujiang color common carp (*Cyprinus carpio var. color*) [16] and *Danio albolineatus* [14], accompanied with a decrease of astaxanthin in skin. However, the erythrophores differentiation and characterization are not well-understood so far.

Thyroid hormone plays a crucial role in regulating metamorphosis in teleost [17–20]. Throughout the metamorphosis process in fish, thyroid hormone induces numerous morphological changes, including eye migration of flatfishes, asymmetric development of body color pattern [17, 18, 21–24]. Previous studies demonstrated the essential role of thyroid hormone in transition of fish larval pigmentation to adult patterns [18, 25]. Interestingly, thyroid hormone has contrasting effects on two classes of neural crest (NCC)-derived pigment cells, reducing melanophores population, while promoting xanthophores development and accumulation of orange carotenoid pigments [19, 26]. The biologically active hormones 3,5,3′-L-triiodothyronine (T3) and thyroxine (T4) [27] exhibit significant effects. Among them, T3 modulates the transcription of specific target genes through thyroid hormone receptors (members of the nuclear receptor superfamily) [28–30], responsible for the pigment cells development and adult pigmentation patterns formation in fish [19, 26, 31]. In clownfishes (*Amphiprion percula*), T3 promotes iridophores production and regulates the formation of white bars [32]. In Neotropical cichlids, thyroid hormones could regulate the formation of black bars and other pattern elements formed by different types of chromatophores [33, 34]. In convict cichlid (*Amatitlania nigrofasciata*) and endler guppy (*Poecilia wingei*), T3 causes the developmental change of asymmetric morphological adult pigment patterns [35, 36]. Although melanophore, iridophore, xanthophore, and erythrophore are differentiated from the neural crest cells [37], the impacts of thyroid hormone on erythrophore development and coloration remain poorly studied.

Spotted scat is a marine aquaculture fish with high economic and ornamental value. There are some studies on the formation of black spots in adults, erythrophore development and pigment identification for red coloration during larval stage [38, 39]. However, the formation of spotted scat pigment pattern during ontogenesis, and the function of thyroid hormone in pigment pattern metamorphosis are unclear. Here, the body color pattern metamorphosis from larvae to adult (whole black-bar-black spot) were explored. In addition, spotted scat

embryos at 0 dpf (day post federalization) and juveniles at 60 dpf were exposed to T3, TU alone or combination with PTU, to reveal the influence thyroid hormone on erythrophores and melanophores development, accumulation of carotenoids, and body color pattern change. Besides, transcriptome sequencing was performed to analyze the molecular effect of thyroid hormone on pigment pattern formation. These results help us to deepen the understanding roles of thyroid hormones in pigment cell development, and provide new insights into thyroid hormone-regulated body color pattern formation in teleosts.

Materials and methods

Treatment experiment design in spotted scat embryos and juvenile

All experimental spotted scat embryos and adults were owned by Donghai Island experimental base of Guangdong Ocean University, and hatched and raised in tanks (30L) in Donghai Island experimental base, Zhanjiang, Guangdong Province. Seawater environment temperature was about 29 ℃. Photoperiod was LD 14: 10 (14-h day/10-h night).

Embryos experiment 1

After fertilization, all embryos were randomly divided into three groups: control group (euthyroid), T3-treated group (hyperthyroid) and TU-treated group (hypothyroid), three replicates per group, 1000 embryos per replicate. Embryos in control group were hatched in natural seawater. Thyroid hormone (T2877, Sigma-Aldrich, St. Louis, MO, USA) was diluted in dimethyl sulfoxide (DMSO) (A503039, Sangon Biotech Co., Ltd. Shanghai, China) to a final concentration at 15 mM [35]. To provoke the hypothyroidism, TU (T8656, Sigma-Aldrich, St. Louis, MO, USA) was dissolved in natural seawater with a final concentration of 2.6 mM [35]. An equal amount of DMSO as in the T3 group was added to both the control and TU-treated group. The seawater containing T3 or TU was changed once a day (every 24 h).

Embryos experiment 2

In spotted scat, erythrophores in skin are gradually covered by melanophores at the embryonic stage. Therefore, to observe the development of erythrophore, melanin was inhibited by 1-phenyl 2-thiourea (PTU) [39]. After fertilization, all embryos were randomly divided into four groups: control, PTU treated (euthyroid group), PTU + T3-treated (hyperthyroid group), and PTU + TU-treated group (hypothyroid group). Each group had three replicates, with 1000 embryos per replicate. In PTU-, PTU + T3- and PTU + TU-treated groups, embryos in tanks were simultaneously treated with PTU (P7629, Sigma-Aldrich, St. Louis, MO, USA), at a standard concentration of 0.003% (200 μM) [40] for 72 h. PTU was dissolved in ethanol, and the seawater was changed daily. The concentrations of T3 and TU used in the treatment were consistent with those in experiment 1.

Embryos in experiment 1 and 2 were treated for 72 h. During hatching, three embryos (biological replicates) were randomly selected and sampled in each group for photographs at 16, 24, 36, 48, 60, and 72 hpf [39].

Juvenile experiment

Spotted scat juveniles were randomly divided into three groups: control, T3- and TU-treated group, and reared in tanks (30 L). All fish in T3- and TU treated groups were expose to 0.1 μg/mL T3 (hyperthyroid group) and 0.02% TU (hypothyroid group) from 60 to 90 dph, and fish in control group were raised in natural seawater. Each group had three replicates, with 20 individuals in each tank. The seawater was changed daily, temperature about 29 ℃, feeding twice a day.

Sample collection and colorimetric evaluation

In the juvenile experiment, in order to maintain region consistency, the red skins (RS), as showed in white dotted line region of Fig. 2A, a″, were collected to analysis the color values and carotenoid content of skin. Black skins (BS) were taken from white box region of Fig. 2A, a. Red and black skin of control, T3-, and TU-treated groups were sampled and stored in an RNA stabilization reagent (Accurate Biology, Changsha, China) for RNA extraction, and stored at -80 ℃ for further pigment analysis. At 90 dph, color values were measured using a CR-400 Chroma Meter (Minolta Camera Co. Ltd., Asaka, Japan). The Chroma Meter was used to measure in L*, a*, and b* values at measurement modes (CIE1976) with the D65 illuminant. The L*a*b* color space (also referred to as CIELAB) is a system for expressing color digitally, developed by the International Commission on Illumination (CIE) in 1976 [41]. In this space, L* (L value) represents the brightness, and its value ranges from 0 (black) to 100 (white). Both a* (a value) and b* (b value) represent the color direction. $a^* > 0$ indicates redness, $a^* < 0$ indicates greenness, $b^* > 0$ indicates yellowness, and $b^* < 0$ indicates blueness [42]. Fish were treated with 10 mg/mL epinephrine (E917252, Shanghai Macklin Biochemical Co., Ltd. Shanghai, China) to contract the pigment before imaging. Photos of pigment pattern and pigment cells development from embryos to juvenile were taken, using a ZEISS microscope with ZEN 3.3 (CARL ZEISS., Ltd. Shanghai, China) and S70 stereomicroscope (Guangzhou Daoyi Science and Technology Co., Ltd. Guangzhou, China).

Spectrophotometry

The total content of carotenoids was measured using absorbance spectrophotometry [43]. Methyl tert-butyl ether (MTBE) (CAS No. 1634–04-4) and NH4OH (CAS No. 1336–21-6) were purchased from Chengdu Chron Chemicals Co., Ltd. (Chengdu, China). Briefly, 0.3 g each sample was used for carotenoid pigment analysis, and the method of pigment extraction was referred to [38, 39]. Finally, using MTBE as a blank control for the carotenoid assay, ultraviolet spectrophotometer (UV-2600A, Unico Instrument Co., Ltd., Shanghai, China) was used to measure absorbance value. The content of carotenoids was determined at absorption wavelengths of 447 nm [44], which was calculated by the following formula:

$$X = A \times K \times V/E \times M$$

X represents the content of carotenoid (mg/kg), A, K and V represent the absorbance value, the constant 10,000 and the volume of fixation (mL), respectively. E and M represent the molar extinction coefficient and the weight of the sample (g), respectively. The extinction coefficient for calculating the content of carotenoids was 2550 [38, 39].

Measurement of thyroid hormones

Each 0.8 g skin sample (three samples per group) were placed into 500 μL of NaCl in a centrifuge tube for homogenization, then centrifugated at 3000 rpm for 10 min, and the supernatant was collected in a new centrifuge tube. The content of T3 and T4 were measured using fish T3 and T4 ELISA Kit according to the manufacturer's instructions (Mlbio. Shanghai, China). Finally, hormone concentration was calculated based on the sample mass.

Total RNA extraction, library construction, and sequencing

Total RNA (three tubes per group) of RS and BS of control, T3-, and TU-treated groups was extracted using Trizol reagent kit (Invitrogen, Carlsbad, CA, USA), according to the manufacturer's instructions. RNA quality assessed on an Agilent 2100 Bioanalyzer (Agilent Technologies, Palo Alto, CA, USA) and checked using RNase free 1% agarose gel electrophoresis. Total RNAs with an RNA integrity number (RIN) score > 7 were selected for sequencing. Eighteen sequencing libraries were constructed and generated by using the NEBNext Ultra RNA Library Prep Kit for Illumina® (NEB, Ipswich, MA, USA) based on the manufacturer's instructions. After treating the samples with DNase I (NEB), messenger RNAs (mRNAs) were isolated by Oligo (dT)-attached magnetic beads (Illumina, San Diego, CA, USA), and then fragmented by fragmentation buffer reagent (NEB). First-strand cDNA was synthesized with fragmented mRNA as a template and random hexamers as primers, followed by second-strand synthesis. Double-stranded cDNA was synthesized using short fragments as templates. AMPure XP beads were applied to select fragments within the size range of 150 bp. Then, 3 μL of USER Enzyme (NEB) was used to select the size, adaptor-ligated cDNA at 37 °C for 15 min, followed by 5 min at 95 °C. PCR was performed using Phusion High-Fidelity DNA polymerase (NEB), universal PCR primers, and Index (X) Primer. Finally, the PCR products were purified by the AMPure XP system, and the quality and quantity of libraries were assessed using the Agilent Bioanalyzer 2100 System and StepOnePlus Real-Time PCR System (Thermo Fisher Scientific, Santa Clara, CA, USA). The index-coded samples were clustered using the cBot Cluster Generation System with the TruSeq PE Cluster Kit v4-cBotHS (Illumina). All cDNA libraries were sequenced on the Illumina NovaSeq 6000 platform.

Data filtering, read mapping, and differential expression analysis

To obtain clean reads, raw reads were filtered using the high-throughput quality control (HTQC) package. High-quality clean data were obtained by filtering reads and removing adapter sequences, and low-quality reads from the Illumina high-throughput sequencing platform and were saved in FASTQ format. All clean libraries were submitted to the NCBI Sequence Read Archive (SRA) database (Accession No.: PRJNA1142162). Based on the spotted scat reference genome sequence (https://ngdc.cncb.ac.cn/search/?dbId=gwh&q=GWHAOSK00000000.1 (accessed on 3 September 2022); accession number GWHAOSK00000000.1), HISAT2.2.4 [45] was used to map RNA-seq clean reads, and String Tie was applied to assemble the mapped reads.

Gene functions were annotated against the NCBI non-redundant (NR; ftp://ftp.ncbi.nih.gov/blast/db/, accessed on 15 January 2024), Swiss-Prot (http://www.uniprot.org/, accessed on 15 January 2024), Kyoto Encyclopedia of Genes and Genomes (KEGG; http://www.genome.jp/kegg/, accessed on 15 January 2024), and Gene Ontology (GO; http://www.geneontology.org/, accessed on 15 January 2024) databases using BLASTx (v. 2.2.26; https://blast.ncbi.nlm.nih.gov/, accessed on 15 January 2024) with an E-value cutoff of $1 \times e-5$.

Gene expression levels were detected using the fragments per kilobase per million (FPKM) method [46]. The DESeq2R package (version 1.16.3) in R (version 3.6.3) [47] was used to identify DEGs. Criteria for screening DEGs were set as $|\log2 \text{ (Fold Change)}| \geq 1$ and FDR < 0.05, where the False Discovery Rate (FDR) refers to the adjusted *p*-value. GO enrichment analysis

of DEGs was implemented using the GOseq R packages (version 1.24.0) based on the Wallenius non-central hyper-geometric distribution [48]. KOBAS (version 3.0) [49] was used to evaluate the enrichment of differentially expressed genes for KEGG pathways. GO terms and KEGG pathways with $p < 0.05$ were considered significantly enriched.

Statistical analysis

Data are expressed as means ± standard error (SE) ($n = 3$). Two-way ANOVA multiple comparisons were used to analyze the genes expression differences with the significance level at $P < 0.05$. Cell number and diameter were analyzed in a quantitative framework using ImageJ software (Rawak Software Inc., Stuttgart, Germany). Statistical analyses were performed using GraphPad Prism 9.0 (GraphPad Software Inc., San Diego, CA, USA).

Results

Development of spot scat body pigments pattern

Larval erythrophores and melanophores were clearly observed during the embryonic stage (Fig. 1A, a, and Fig. S1A). After hatching, the body trunk was gradually covered by larval melanophores (Fig. 1A, b-d). Until 8 dpf, larval erythrophores appeared in the upper behind of head (Fig. 1A, e), and iridophores emerged on the eye socket and operculum at 14 dpf (Fig. 1A, g-h). From 25 to 90 dpf, the red bars and spots were formed and mainly filled with adult erythrophores, which were mainly distributed on the upper of head, base of the first dorsal fin, joint of the first and second dorsal fin, joint of second dorsal, and caudal fin, and caudal fin of spotted scat (Fig. 1A, i-p). Meanwhile, the body trunk was almost covered with adult melanophores at 25 dpf (Fig. S1B). From 25 to 45 dpf, the pigment pattern of spotted scat juvenile changed from the whole-body black color (Fig. 1A, i) to black spaced vertical bars, with first and second black bar formed at 33 dpf, and third one formed at 45 dpf (Fig. 1A, j). Ultimately, three black spaced vertical bars from dorsum to abdomen of body trunk were observed (Fig. 1A, j-k). From 60 and 65 dpf, black spots were gradually appeared between each black spaced vertical bars (Fig. 1A, l). From 65 to 90 dpf, these black vertical bars gradually transformed into black spots (Fig S1B, h). Simultaneously, the red color of bars and spots gradually bleached out, and transformed into yellow color, which was mainly consisted of adult xanthophores (Fig. 1A, p). These black spots were formed in spotted scat at 90 dpf, maintained throughout their life. The body pigment pattern development progress of spotted scat was showed in Fig. 1B. During the progress, larval erythrophores and melanophores were simultaneously observed form 0 dpf, iridophores were appeared from 14 and 65 dpf, respectively (Fig. 1C). In the late juvenile and adult pigment pattern, the population of erythrophores was replaced by the yellow-orange xanthophores (Fig. 1B, 1C, and Fig S1B, g). The definitive pattern of spotted scat is mainly formed by three adult chromatophore lineages: melanophores, iridophores, and xanthophores.

Effects of TH on pigment development

The levels of T3 and T4 in T3 treatment group were higher than control and TU treatment group, while the lowest level in the TU treatment group (Fig. 2B, C). The body weight and length of spotted scat in TU treatment group were significantly lower than those of control and T3 treatment groups (Fig S2B, 2C). While the number of black spots was significantly reduced in T3-treated group (Fig. 2A, b), compared with the control and TU groups (Fig. 2D). Simultaneously, the population of melanophores on the black-spotted (white box) and non-spotted skin (red box) decreased after T3 treatment (Fig. 2A, b, E and Fig S2A, S2D). When thyroid hormone synthesis was suppressed by administration of TU, the melanophore population of non-spotted skin increased significantly (Fig S2D, c and Fig. 2E). Similarly, in spotted scat larvae, population of melanophores were reduced in T3 treatment group, with the smaller size pigment granule than control and TU treatment group (Fig S3). In contrast, dorsal iridophores were increased in the T3 treatment group (Fig. 2A, b), whereas iridophores were barely visible in the TU treatment group (Fig. 2A, c). In the T3 treatment group, red coloration of the skin on the head was significantly weakened (Fig. 2A, b). For chromatic aberration value analysis, both L and b value of spotted scat non-spotted skin in T3 group were significantly higher than those of control and TU groups, except for a value (Fig. 2 F, 2G, 2H). Surprisingly, the concentration of carotenoids in spotted scat skin was increased after treatment with TU, compared with T3 groups (Fig. 2I). There was no significantly change in the pigmentation pattern 12 days after cessation of hormonal treatment at the juvenile stage, and the change in body color patterns may need to be observed over a longer period of time (Fig S2E).

Illumina sequencing and annotation, functional enrichment analyses of differentially expressed genes (DEGs)

In this study, black (BS, white box region in Fig. 2A, a, b, c) and red skin (RS, white dotted line region in Fig. 2A, a, b, c) of spotted scat juvenile in control, T3 and TU treatment groups were sampled and chosen for RNA-Seq analysis. Eighteen skins cDNA libraries were constructed from above three groups. After quality control of sequencing data, 751,357,836 clean data were obtained.

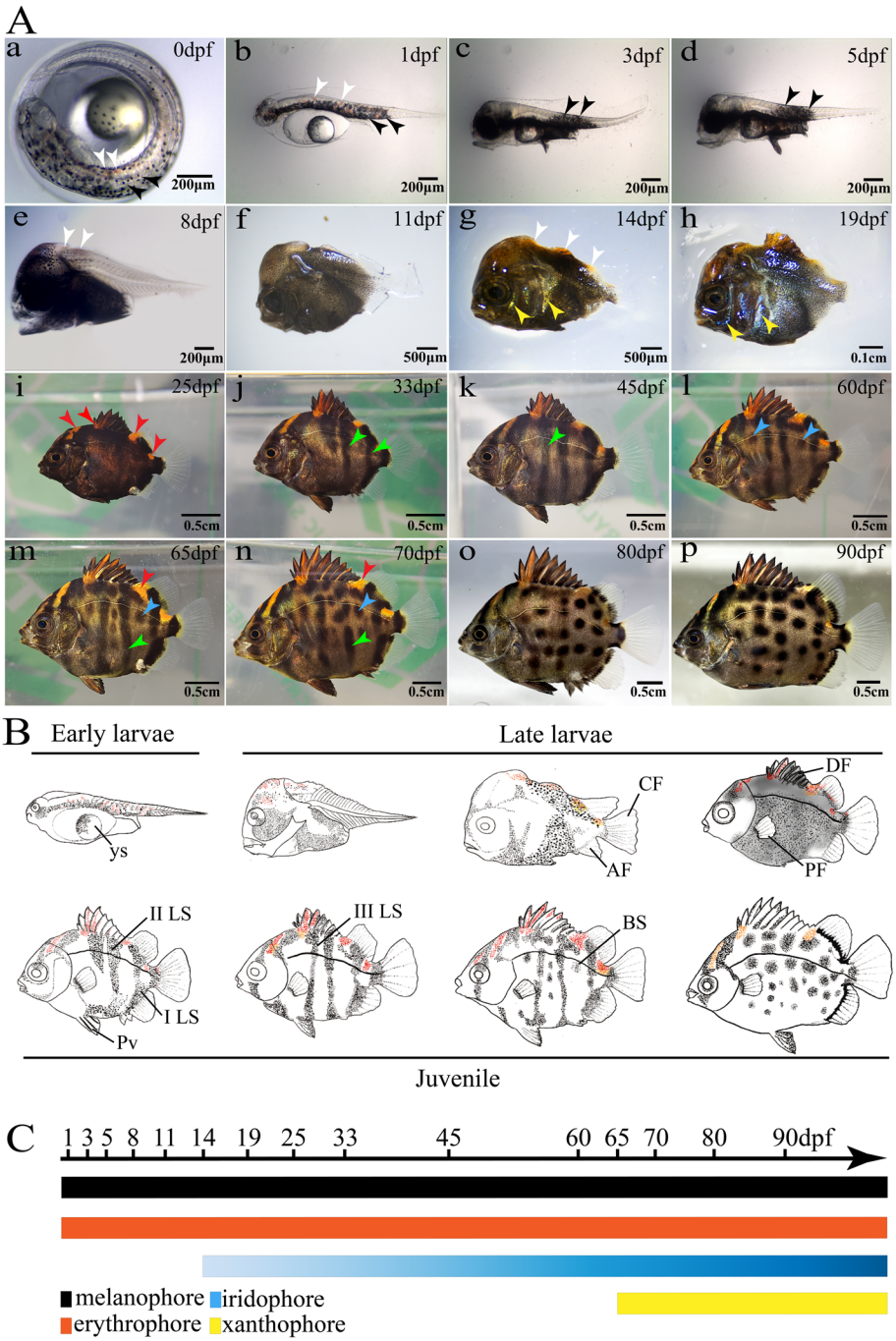

Fig. 1 Development of body pigments pattern in spotted scat. **A** Body pigments pattern at different development stage. (a) embryonic stage, (b, c, d) early larval stage, (e, f, g, h, i) late larval stage, (j, k, l, m, n, o, p) juvenile stage. The white and black arrows indicate erythrophores and melanophores, respectively. The yellow and red arrows indicate iridophores and red spot, respectively. The green and blue arrows indicate black bars and spots, respectively. **B** Diagram of spotted scat body pigments pattern development. ys, yolk sac; pc, pericardial cavity. I, II and III LS, first, second and third black vertical bars. A, anal fin; C, caudal fin; D, dorsal fin; Pv, pelvic fins; BS, black spot. dpf, day post fertilization. **C** Sequence of different pigment cells appearance in spotted scat

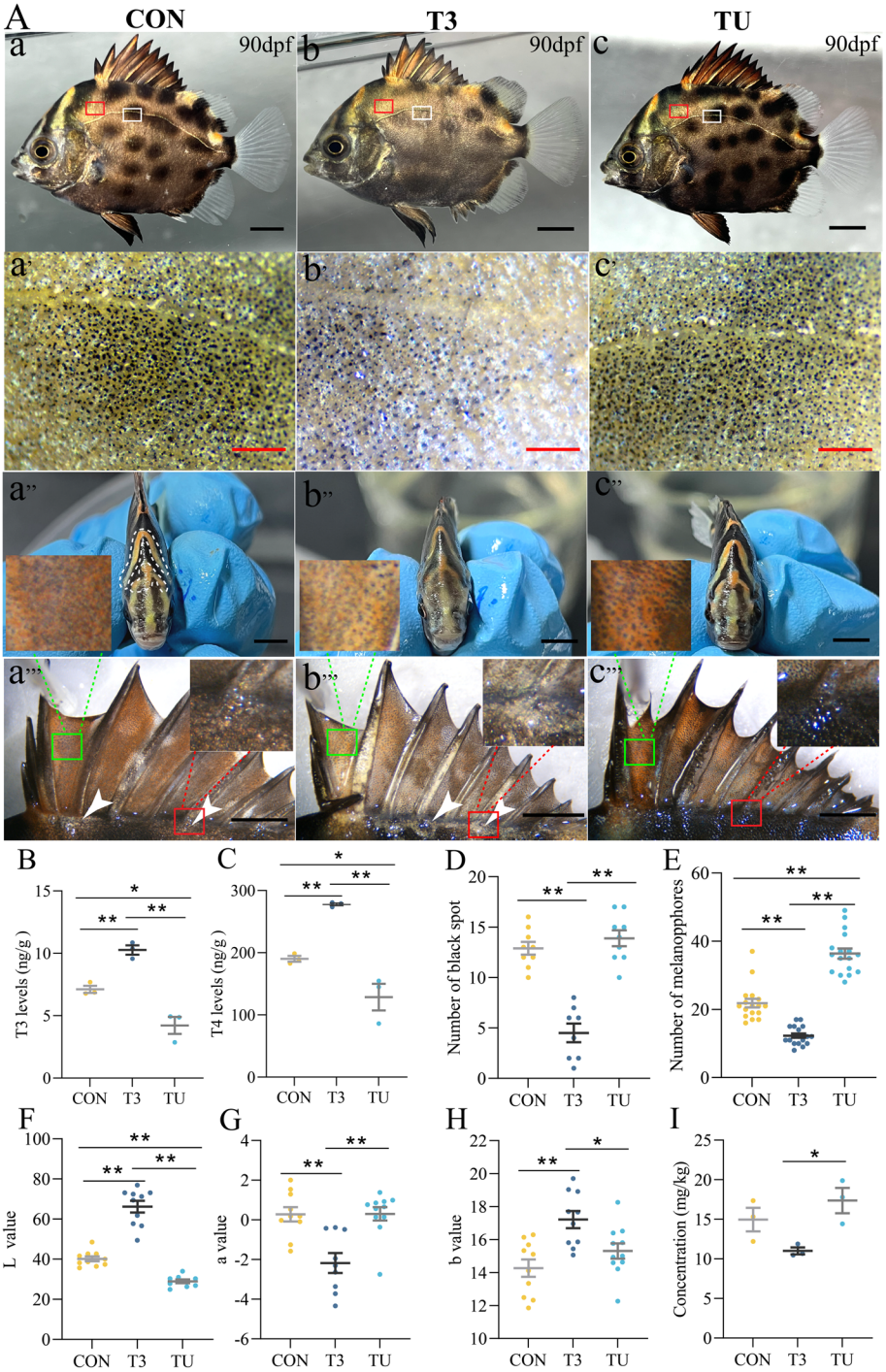

Fig. 2 Characteristics of body pigments pattern in spotted scat treated with different T3 and TU. **A** (a) control group, (b) T3 treatment group, and (c) TU treatment group. (a,, b,, c,,) Comparison of melanophore in control, T3, and TU treatment group after epinephrine treatment. The regions were the white box area in a, b, and c, respectively. (a,,, b,,, c,,) Characteristics of the head in control, T3, and TU treatment group, respectively. (a,,,, b,,,, c,,,) Characteristics of the dorsal fin in control, T3, and TU treatment group, respectively. Scale bar of a, b, c, a,,, b,,, c,,, a,,,, b,,,, and c,,, 0.5 cm, scale bar of a,, b,, and c,, 200 μm). **B** T3 levels (ng/g). **C** T4 levels (ng/g). **D** Number of black spots. **E** Number of melanophores (4×10^{-2} mm2). **F**, **G**, and **H** Brightness: L value, redness/greenness: a value, and yellowness/blueness: b value. **I** Concentration of carotenoids (mg/kg). The symbols "*" and "**" above the error bars indicate significant differences at the levels of $p = 0.05$ and $p = 0.01$, respectively

Table 1 Statistics of RNA sequencing data

Samples	Raw Data	Clean Data (%)	Q30 value (%)	GC Content (%)
CON-BS-1	36,829,388	36,564,624 (99.28)	95.25	48.22
CON-BS-2	41,443,434	41,126,556 (99.24)	95.28	48.67
CON-BS-3	43,211,674	42,897,046 (99.27)	95.19	48.49
T3-BS-1	37,376,494	37,082,210 (99.21)	95.38	48.37
T3-BS-2	43,532,050	43,190,250 (99.21)	95.43	48.38
T3-BS-3	36,328,664	36,078,220 (99.31)	95.59	48.04
TU-BS-1	37,412,544	37,136,788 (99.26)	95.46	48.06
TU-BS-2	41,188,466	40,895,130 (99.29)	95.41	48.14
TU-BS-3	43,729,508	43,474,838 (99.42)	95.79	48.42
CON-RS-1	45,381,110	45,086,768 (99.35)	95.61	47.85
CON-RS-2	36,997,450	36,744,630 (99.32)	95.66	48.03
CON-RS-3	43,844,520	43,558,058 (99.35)	95.51	48.01
T3-RS-1	41,767,040	41,478,020 (99.31)	95.35	48.10
T3-RS-2	36,610,402	36,354,814 (99.30)	95.28	48.29
T3-RS-3	54,780,924	54,410,058 (99.32)	95.38	48.20
TU-RS-1	39,622,746	39,353,836 (99.32)	95.27	48.42
TU-RS-2	53,484,488	53,301,690 (99.66)	96.68	48.24
TU-RS-3	42,917,396	42,624,300 (99.32)	95.56	47.82

Samples: sample name; Raw Data: counts of raw reads; Clean Data: total length of clean data; ≥ Q30 percentage of bases with a Q-score of no less than Q30. GC content: percentage of G and C bases in clean data. Black skin samples of spotted scat in control (CON-BS), T3 (T3-BS) and TU treatment group (TU-BS), Red skin samples in control (CON-RS), T3 (T3-RS), TU treatment group (TU-RS)

The GC content and Q30 values excess 47% and 95%, respectively (Table 1).

Principal component analysis (PCA) was performed to investigate the consistency in gene expression profiles among control, T3 and TU treatment groups. All biological replicates were aggregated, and the different treatment groups were clearly separated, the first and second principal components (PCs) displayed 50.1% and 17.8% total variance, respectively (Fig. 3A). In addition, 203 and 204 co-expressed genes showed significant expression differences in BS and RS groups, respectively (Fig S4A, S4B).

KEGG pathways enrichment analysis showed that DEGs were notably presented in DNA replication, cytokine-cytokine receptor interaction, viral protein interaction with cytokine and cytokine receptor, and hypertrophic cardiomyopathy in all groups. Here, we focused on pigment synthesis pathways, especially in melanin and carotenoid metabolism. In CON-BS-vs-TU-BS group, enrichment pathways, including vitamin B6 metabolism, retinol metabolism, tyrosine metabolism, and melanogenesis, were found to be closely associated with carotenoid and melanin synthesis (Fig S5B). The Wnt signaling pathway, and thyroid hormone synthesis, involved in pigment cell differentiation, were significantly enriched in T3-BS-vs-TU-BS and CON-RS-vs-T3-RS groups, respectively (Fig S5C, 5D). Furthermore, in CON-RS-vs-TU-RS and T3-RS-vs-TU-RS groups, DEGs were significantly enriched in vitamin metabolism pathways, such as vitamin digestion and absorption and vitamin B6 metabolism (Fig S5E, 5F).

By genes expression pattern, function annotation and pathway enrichment analysis, some important DEGs associated with thyroid hormone signaling pathway were further investigated in black and red skins. Of them, *tpo* and *tg* displayed the low expression in both black and red skin, with the down-regulation of *tpo* mRNA expression in TU treatment group (Fig. 4A). Iodothyronine deiodinase encode gene *dio3* mRNA expression was significantly increased in skins of T3 treatment group, compared to the control and TU treatment group, while *dio1* and *dio2* mRNA showed low expression in skins, with no significant difference between the three groups (Fig. 4A, B). Besides, the expression of thyroid hormone receptor gene *thra*, *thra-l* was highly stimulated in skins of spotted scat in TU treatment group, compared to the control and TU treatment groups (Fig. 4A, B). Gene associated with melanophore and melanogenesis were significantly higher in TU treatment group, including *tyr*, *tyrp1*, *dct*, *oca2*, *pmel*, *slc24a5*, *slc7a11*, *erbb3* and *mitf* (Fig. 5A). In BS, the expression of genes, related to iridophore differentiation (*fhl2-l*, *fhl2*, *ltk*, *id2a*, and *alx4*) and guanine synthesis (*gmps*, *hprt1*, *ppat*, *impdh1b*), were stimulated by T3 treatment, but down-regulated by TU treatment (Fig. 5B). Additionally, genes related to pteridine synthesis, carotenoid transport and deposition, such as *apod*, *pnpla2*, *wu:fc46h12*, *rdh12*, *stard10*, *xdh*, *gch2*, *abca1*, *retsat*, *scarb1*, *spr*, *rgs2*, *bco2*, *ttc39b* and *rbp7* (Fig. 5C), exhibited the down-regulated expression pattern in skins of T3 treated spotted scat, and showed the up-regulated trend in TU treatment groups.

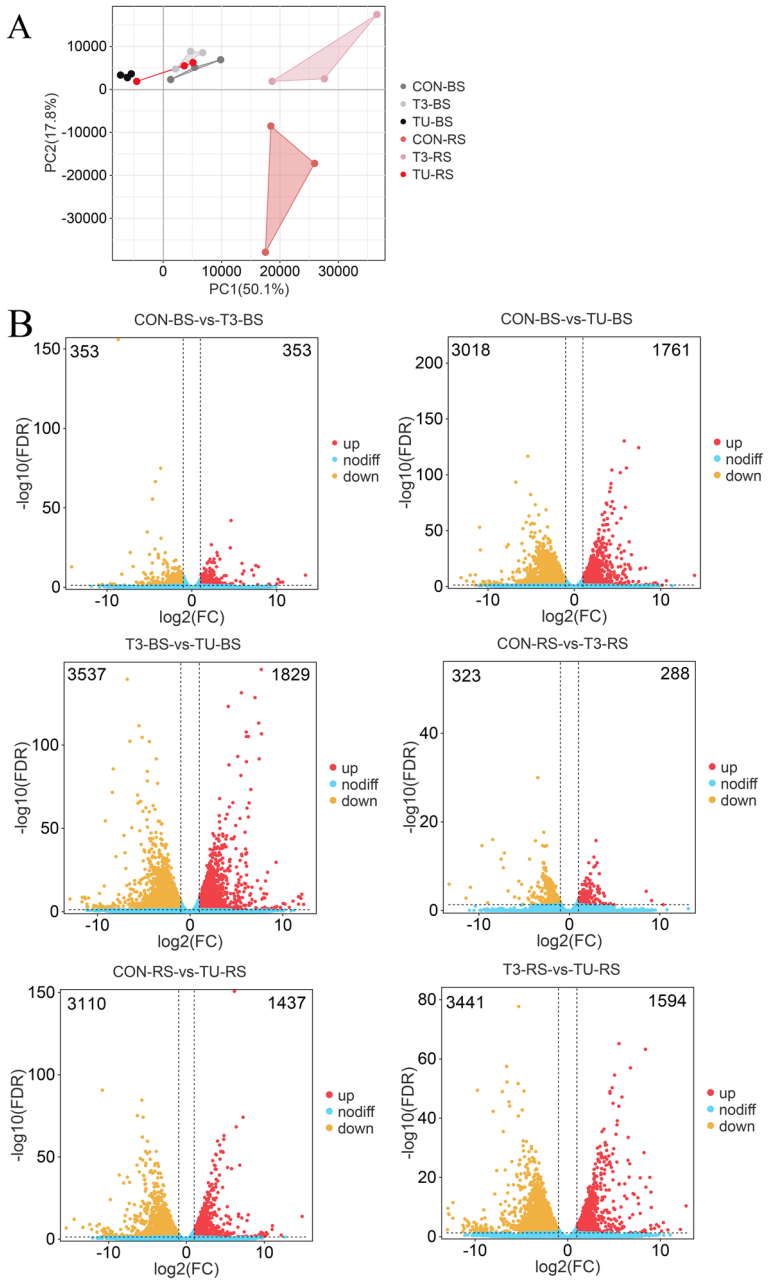

Fig. 3 Differentially expressed genes analysis of spotted scat skins in different treatment group. **A** Principal component analysis of the 18 datasets. **B** Volcano plots of six paired wise comparisons. The up-regulated and down-regulated DEGs are shown using red and yellow dots, respectively. DEGs were set as |log2 (Fold Change)|> 1 and FDR < 0.05

Effects of thyroid hormone on erythrophores morphology and number

Following_treatment with TU, the expression levels of genes associated with xanthophore, pteridines and carotenoids were significantly up-regulated in spotted scat skin. To assess the influence of T3 and TU treatment on erythrophore development, spotted scat embryos were treated with T3, TU, and PTU (0.003%) in combination, which is known to inhibit melanin formation. Firstly, spotted scat embryos were treated with different concentrations of PTU alone, the number and size of larval erythrophore were not significantly changed, eliminating the potential impact of PTU on erythrophores (Fig S6). Embryos in control group were treated with the ethanol without PTU, microscopic observation showed that larval erythrophores were

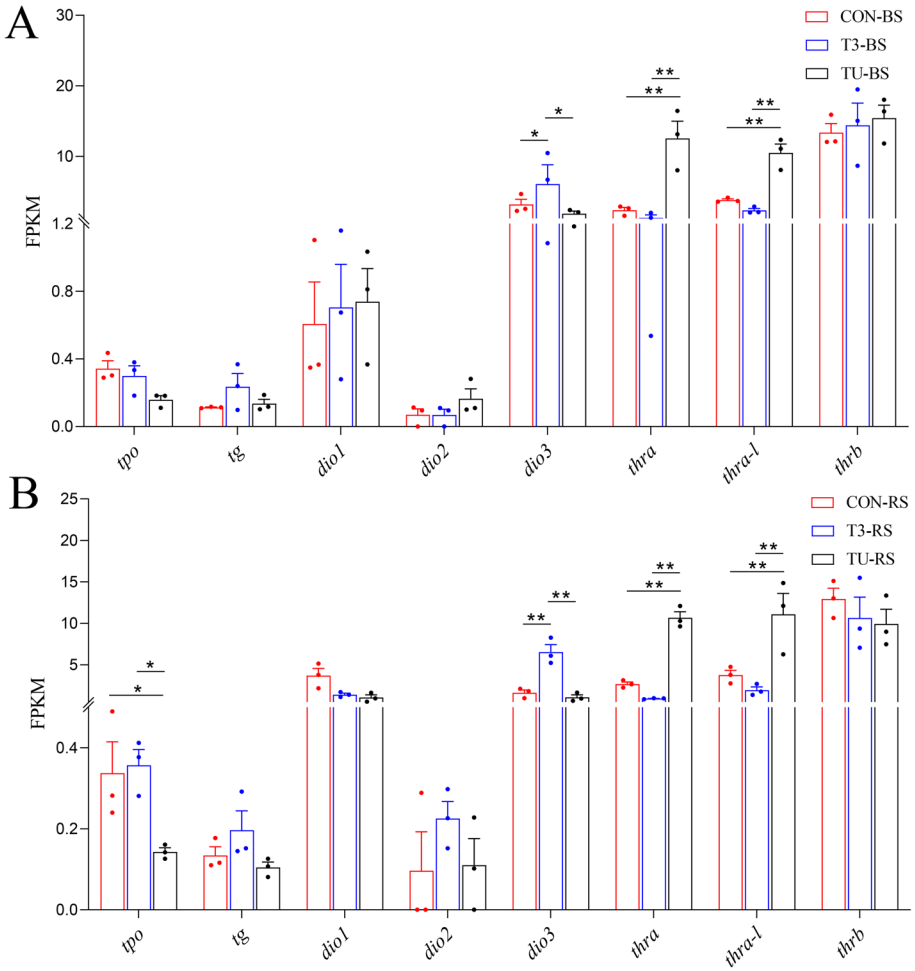

Fig. 4 Expression pattern of thyroid hormones signaling pathway genes in black (BS) and red skins (RS) of spotted scat across different treatment groups. **A** DEGs associated with thyroid hormones signaling pathway in BS. **B** DEGs associated with thyroid hormones signaling pathway in RS. The symbols "*" and "**" above the error bars indicate significant differences at the levels of $p=0.05$ and $p=0.01$, respectively

distributed in trunk at 16 hpf, then gradually covered by the increasing larval melanophores (Fig S7, a-f). In PTU, PTU + T3 and PTU + TU groups, more and more larval erythrophores appeared and distributed in head, eyes, and trunk from 16 to 36 hpf, and decreased in trunk and assembled in venter from 48 to 72 hpf (Fig. 6, a-r, and Fig S7, g-x). Obviously, compared to PTU and PTU + TU group, less larval erythrophores were visible in PTU + T3 treatment group from 48 to 72 hpf (Fig. 6, j-l). In PTU + T3 treatment group, number of larval erythrophores was less than PTU and PTU + TU treatment group at 24 hpf, and reduced rapidly from 36 to 72 hpf (Fig. 7A). The diameter of larval erythrophores in PTU + T3 treatment group was significantly smaller than that in PTU, and PTU + TU treatment groups from 16 to 72 hpf (Fig. 7B).

Characteristics in spotted scat of PTU (a-f), PTU + T3(g-l), and PTU + TU (m-r) treatment groups during embryos development. Erythrophores are indicated by white arrows. Scale bar, 200 μm.

Expression trends of genes related to pigment cells differentiation (melanophore, erythrophore, and iridophore) and their substance metabolic pathways (melanin, carotenoid, pteridine, and guanine) under T3 changes in spotted scat. Red marker gene of melanophore/melanin and erythrophore/carotenoid were up-regulated in response to T3 inhibition, but red marker gene of iridophore/guanine were up-regulated by excess T3, grey arrows represent possible regulatory roles.

Discussion

Pigment pattern development in spotted scat

In many animals, color patterns play the crucial roles in species communication, such as species recognition, mate choice and camouflage [50]. Some apparent morphological transformation undergoes during ontogeny

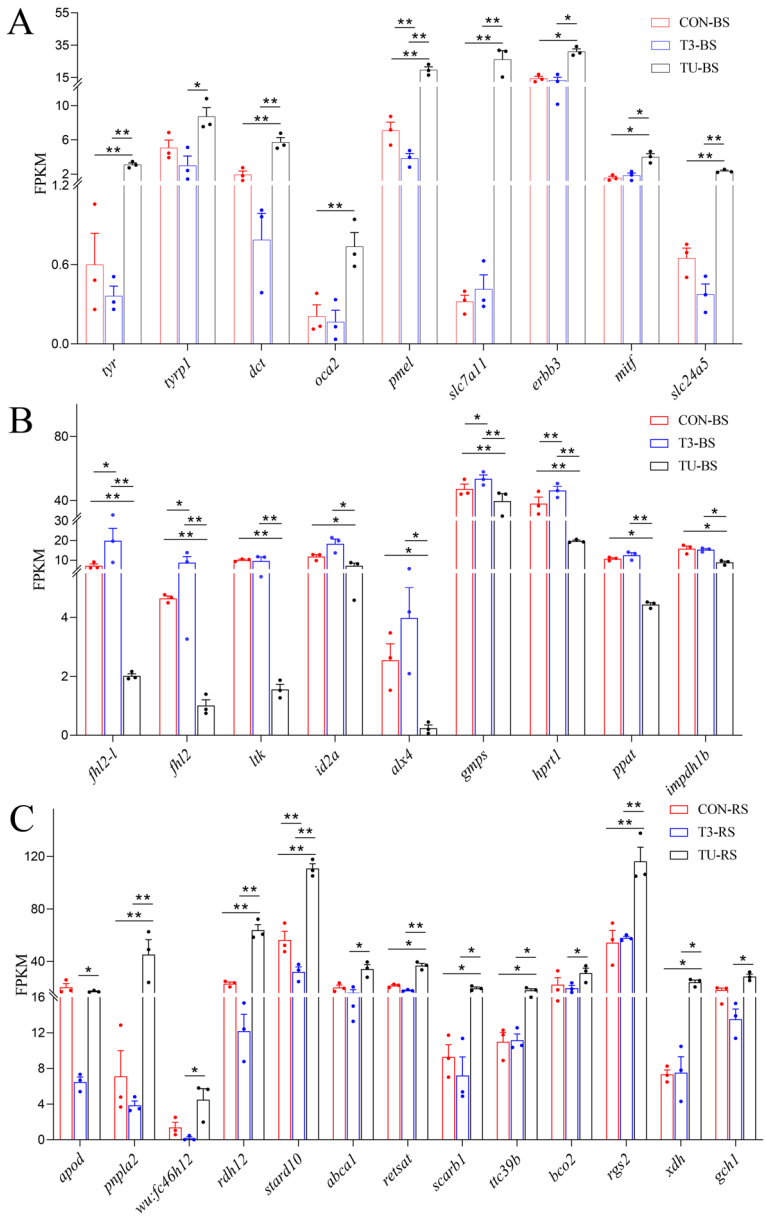

Fig. 5 Expression pattern of pigment cell differentiation and pigment synthesis in black (BS) and red skins (RS) of spotted scat across different treatment groups. **A** DEGs associated with melanophore and melanin synthesis in BS. **B** DEGs associated with iridophore differentiation and guanine synthesis in BS. **C** DEGs associated with carotenoid transport and deposition, and pteridine synthesis in RS. The symbols "*" and "**" above the error bars indicate significant differences at the levels of $p = 0.05$ and $p = 0.01$, respectively

[51], including the type and ratio of chromatophores, distribution, and changes of pigment composition [18, 52] thereby transforming pigment patterns. Stripes, bars and spots are common basic body color patterns in teleost, appearing at different developmental stages and forming the final pattern in adults. In some cichlids from Lake Malawi and East African, the development of bar, stripe and spot pattern has been described [2]. The body color pattern in adult cichlids is predictable and same as that of juvenile fish. In *Copadichromis azureus* and *Dimidiochromis compressiceps*, the stripe, bar, and spot chromatophores appear in skin during metamorphosis, and melanophores in stripe differentiate into the adult pattern along the horizontal myosepta [2]. In adult zebrafish, the formation of pigment stripe is influenced by the interactions of pigment cells and environment factor [53]. The elegant stripe patterns in adults zebrafish emerge during the juvenile stage and are composed of melanophores,

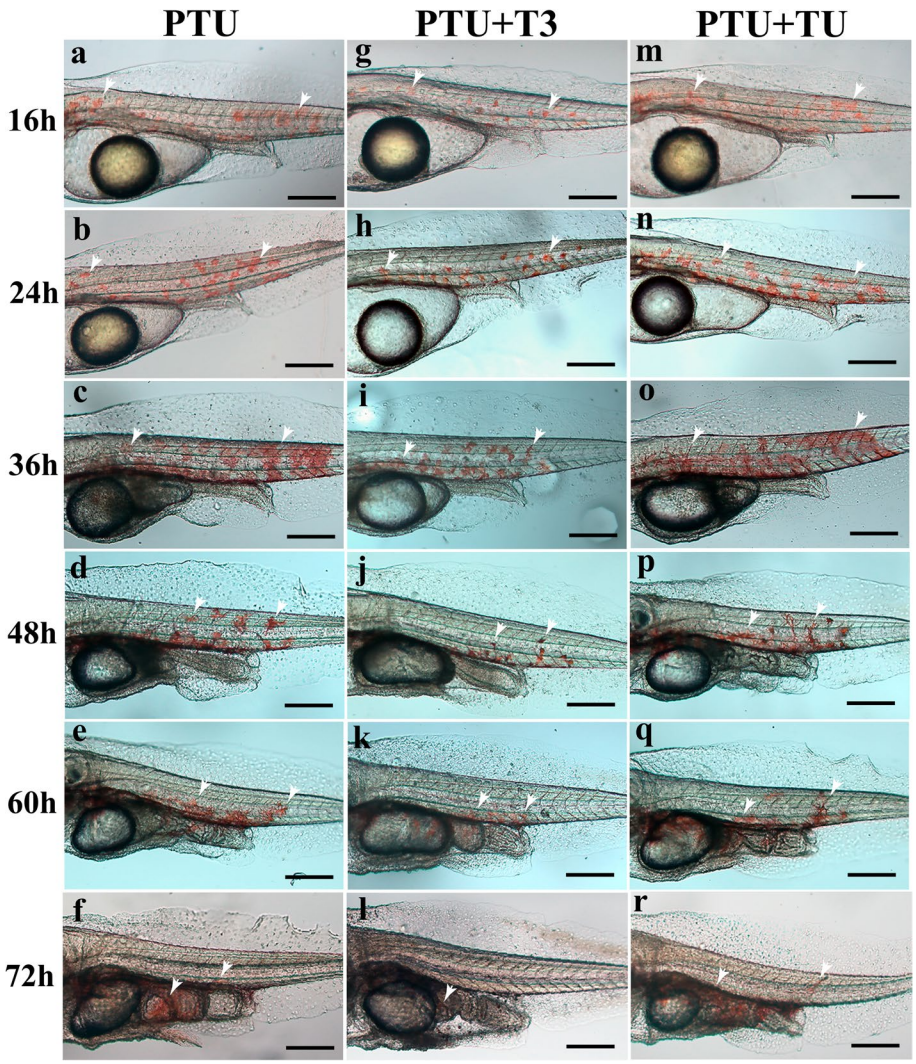

Fig. 6 Distribution changes of erythrophores in spotted scat under different hormonal treatments during embryos development

xanthophores, and iridophores, which organize into intricate patterns [19, 54, 55]. In spotted scat, the pigment pattern can be categorized into four stages after hatching: early larvae, late larvae, juvenile, and adult stage. The bar formed during the transition from larvae to juvenile stage, subsequently transforming into the black spots and maintained throughout the whole adult stage. Both patterns consist of a large number of melanophores, distinguishing from the complex pigment cell composition in zebrafish. Although spots and bars are classical pigmentation patterns, body color pattern in spotted scat undergoes complex metamorphic transformations. It started with the appearance of larval erythrophores and melanophores during the embryonic stage, followed by iridophores, and concluded with the emergence of adult xanthophores. Meanwhile, melanophores and erythrophores showed a pattern of increase followed by decrease in spotted scat, consistent with our previous study [39]. We have conducted a preliminary study on the process of body pattern formation in spotted scat, but the molecular regulatory mechanism remains unknown.

The function of thyroid hormone signaling on body coloration

Pigment patterns formation, such as stripes, bars and spots, is the classic and basic scientific question, which attracted the sustained attention of many researchers [56]. Thyroid hormone signaling plays important roles in pattern formation during metamorphosis [18] and larval pigmentation transformation toward the adult pattern in teleosts [25]. In juvenile Japanese flounder (*Paralichthys olivaceus*) [57] and adult zebrafish [19, 31], thyroid hormone T4 treatment could inhibit the formation of melanophores. In some cichlid species, thyroid hormone alters

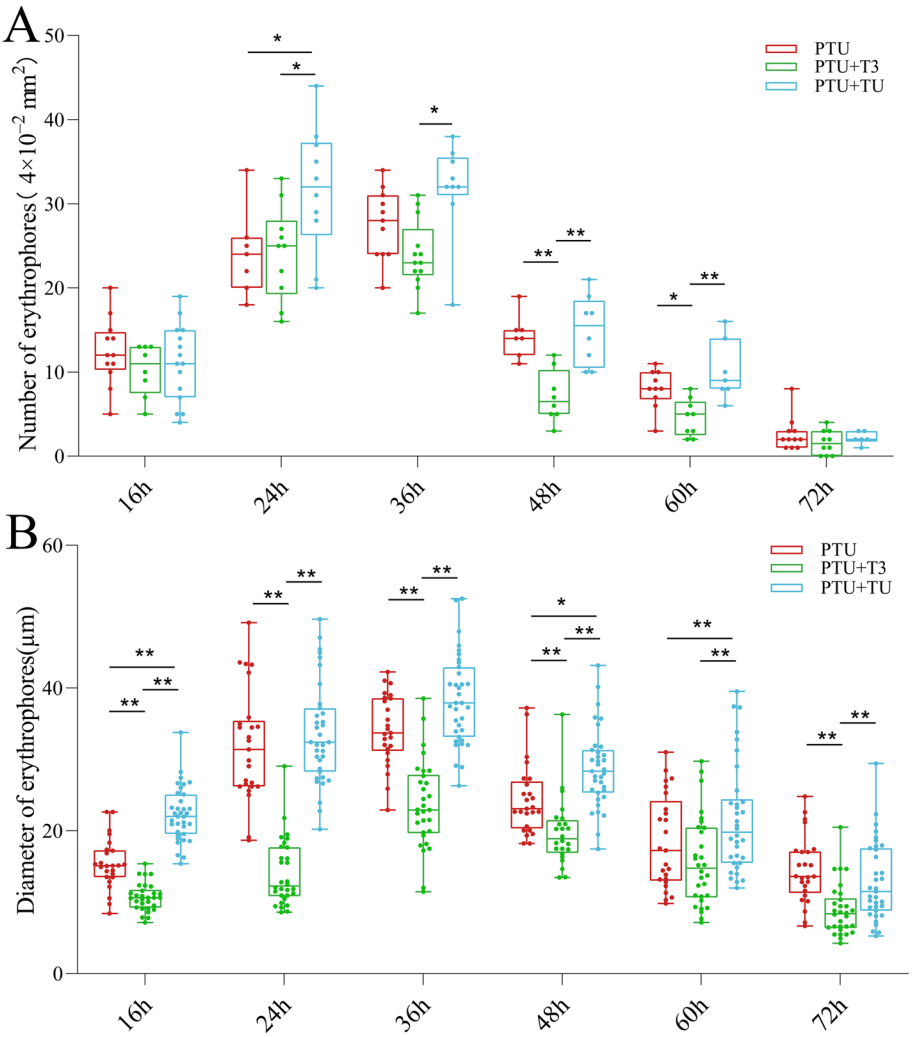

Fig. 7 Number and diameter changes of erythrophore in spotted scat under different hormonal treatments during embryos development. **A** and **B** Cells number and diameter of larval erythrophores at different embryo development stages. The symbols "*" and "**" above the error bars indicate significant differences at the levels of $p = 0.05$ and $p = 0.01$, respectively

the final adult pattern by influencing the elements of the pigment pattern. For example, during the metamorphic transformations of pigment pattern in the convict cichlid *Amatitlania nigrofasciata*, reduction of thyroid hormone signaling leads to an increased number of bars [35, 36]. In this study, T3 and T4 levels were increased in adult pigment pattern spotted scat of the T3 treatment group, while they decreased in the TU treatment group. As expected, thyroid hormone treatment inhibited the formation of adult melanophores from bar to spot stage, as well as embryonic melanophores. Following the suppression of thyroid hormone signaling, although the number of spots did not increase, there was a significant rise of in the melanophores number. These results suggested that the formation of melanophores and transformation of pigment patterns were stimulated by the disruption of thyroid hormone signaling, while they were suppressed by the activation of thyroid hormone signaling. However, the molecular suppression effect of thyroid hormone on melanophore is still unclear.

In this study, transcriptomic analysis showed that DEGs such as *tyr*, *tyrp1*, *dct mitf*, *pmel*, and *oca2* were significantly enriched in pathways, associated with melanin synthesis and Wnt signaling pathway. Tyrosinase (TYR), tyrosinase-related protein1 (TYRP1) and dopachrome tautomerase (DCT) belong to melanophore-specific gene family, and involved in melanin synthesis [8]. Knockout of *tyr* and *tyrp1* gene in fish causes the disruption of melanophore formation [58–60]. During melanophores development, the expression of tyrosinase family

genes is thought to be orchestrated by binding of MITF in some degree. MITF is essential for the melanophore cell-fate determination during commitment from pluripotent progenitors in the neural crest, and function as a potent specific transcriptional regulator of three major genes (*tyr*, *tyrp1*, and *dct*), as well as other pigmentation genes [9]. In this study, both the expression of *mitf* and its downstream genes *tyr*, *tyrp1* and *dct* were up-regulated after TU treatment, consistent with the induce of melanophores formation. In vertebrates, *pmel* is a critical gene for melanin biosynthesis. In mice, mutation of *pmel* gene affects the shape of melanosomes [13]. Furthermore, *oca2*, also known as the pink-eyed dilution gene or melanophore-specific transporter gene, is necessary for trafficking melanosomes. In fish, mutation of *oca2* results in the serious albinism [10–12]. Solute carrier 24 member (*slc24a5*) is a melanosomal ion transport protein, albinism and hypopigmentation defects were observed in *slc24a5*-knockout mice [61] and KawaKawa (*Euthynnus affinis*) [62]. The receptor tyrosine kinase gene *erbb3* is essential for melanophore development [63]. In this study, above genes related to melanogenesis showed the up-regulated expression pattern after disrupting the thyroid hormone by TU, accompanied with the increased melanophores. These results suggested thyroid hormones repress melanophores formation by inhibiting melanin synthesis. Unexpectedly, T3 treatment caused the reduction of melanophores number and diameter, however, the expression of genes associated melanin synthesis was not changed. KEGG pathways analysis of CON-BS-vs-T3-BS group found that DEGs was enriched in autoimmune thyroid disease. Previous report has highlighted thyroid diseases (TD) would lead to the autoimmune skin diseases (AISD) such as vitiligo [64], similar to the abnormal and irregular skin coloration pattern in T3-treated spotted scat. Additionally, thyroid hormone signaling has been demonstrated to involve in cellular oxidative-stress responses and cell damage/death of the retinal pigment epithelium (RPE) cells, and the deficiency of thyroid hormone receptor (THR) protected the cell of RPE from death [65]. In *Xenopus tropicalis*, THR-α mediated in cell cycle programs activated by T3, which was involved in larval epithelial cell death and adult epithelial stem cell development during intestinal remodeling [66]. Meanwhile, the THR target genes are mainly enriched in cell cycle-related biological pathways, and THR-α knockout could significantly reduce the enrichments. More importantly, T3-induced intestinal remodeling was blocked by the inhibited cell cycle [67]. These results were consistent with KEGG pathways analysis of spotted scat skin transcriptome in this study, and DEGs was enriched in cell cycle of both CON-BS-vs-TU-BS and T3-BS-vs-TU-BS groups. Therefore, we suggest that the excess thyroid hormone treatment caused the reduction of melanophores number and diameter, death of melanophores and body color pattern remodeling during metamorphosis.

In teleost, melanin (melanophores), pteridine (xanthophores), and guanine (iridophores) pigments can be synthesized autonomously [68, 69], carotenoids cannot be synthesized by fish and need to be obtained from food. Thyroid hormone can inhibit melanophore formation [19, 31, 57, 70], promote the proliferation of xanthophore and iridophore [19, 26, 32, 35]. In spotted scat, iridophores were significantly increased after T3 treatment, and the expression level of the iridophore differentiation gene *fhl2-l*, *fhl2*, *ltk*, *id2a*, *alx4* [71, 72] were strongly increased in T3 treatment group, but decreased in TU treatment group. Furthermore, guanine synthesis pathway gene (*gmps*, *hprt1*, *ppat*, *impdh1b*) were up-regulated after T3 treatment, but down-regulated after TU treatment, indicating that thyroid hormone promotes the increase of iridophore by promoting the expression of genes related to iridophore differentiation and guanine synthesis. This is consistent with the results in clownfish, where thyroid hormones promote the proliferation of iridophore and white bar formation [32]. In xanthophores, thyroid hormone could upregulate the expression of *scarb1* (scavenger receptor class B, member 1) gene, promoting the accumulation of β-carotene and making the cells visible [26]. In spotted scat juvenile fish, although T3 treatment increased the brightness (L value) and decreased the redness (a value) of skin, the accumulation of carotenoids in red skin of spotted scat was not changed. However, the carotenoids content was significantly increased in TU treatment fish. Our previous study revealed that β-carotene was the main pigment, contributing to red coloration in erythrophores of spotted scat [39]. These results implied that disruption of thyroid hormone signaling might enhance the erythrophores development in spotted scat. In order to explore the function of thyroid hormone in regulating erythrophores development, spotted scat embryos were treated with T3, TU in combination with PTU. T3 treatment caused the less larval erythrophores appeared in spotted scat, accompanying with the reduced number and smaller diameter of larval erythrophores in T3 treatment group than control and TU treatment group. The reduction of larval erythrophores diameter induced by T3 treatment was similar to the epinephrine caused pigment granules to contract toward cell centers [14]. Above results showed that thyroid hormone signaling could inhibit erythrophores formation and suppress carotenoids accumulation in spotted scat, and the regulatory function among different lineage cells seems to be distinguishing. Furthermore, during the juvenile-adult transition stage, when the red–orange model elements were formed, the fish

were treated with hormones for only 30 days, and 72 h of limited treatment in the early stages of development. Therefore, if thyroid hormone treatment was started and last for a long time at the larval and juvenile stage, other phenotypic consequences are likely to occur, including changes in melanization patterns and pattern elements formed by formed by erythrophores and xanthophores. This aspect remains a subject for further study.

Red coloration is a valuable economic trait and serves as an honest signal of individual quality in mate choice, and dominated by erythrophores [73, 74]. In this study, the molecular mechanism of thyroid hormone in regulation erythrophores development and red coloration was revealed by transcriptome analysis. DEGs related to carotenoid metabolism, lipid metabolism, and pteridine synthesis, such as *abca1* (ATP-binding cassette A1), *stard10*, *apod*, *pnpla2*, *rdh12*, *scarb1*, *xdh*, and *gch1* were identified. The metabolic process of carotenoids was divided into three steps, including uptake and transport, binding, deposition, and breakdown. In aquatic animals, *scarb1* was a crucial scavenger receptor for carotenoid uptake, both *scarb1* mutant of *Danio albolineatus* and Oujiang color common carp lose their red coloration, with the decreased carotenoid in skin [14, 16]. Transport proteins gene *abca1* is involved in carotenoids transport, and possesses the broad substrate specificity [75]. Additionally, *apod* was involved in carotenoids binding and deposition [76, 77]. In golden pheasant (*Chrysolophus pictus*) plumage, *apod* was identified as a candidate gene for red coloration [78], and was relevant to erythrophore formation during embryonic development of spotted scat [39]. Furthermore, in red tilapia (*Oreochromis spp.*), except for *apod* and *scarb1*, *stard10*, *pnpla2* (Patatin-like phospholipase domain containing 2), and *rdh12* were also involved in carotenoids metabolism, cooperated with lipid metabolism, and they showed high expression levels in red skin [15]. And *rdh12* was thought to be involved in the enzymatic pathway of *bco2*-based spectral filtering of carotenoids, and sufficient to the production of dihydrogalloxanthin from zeaxanthin [79]. In an East African cichlid fish (*Tropheus duboisi*), *pnpla2* plays the critical roles in regulating triglyceride lipid catabolic process, and functions as a candidate carotenoids coloration gene [80]. In this study, above six genes expression was significantly stimulated when the thyroid hormone signaling was inhibited using TU. These results implied that thyroid hormone signaling affected red coloration in spotted scat, through regulating the carotenoids metabolic process. In our previous study, we have demonstrated that pteridine was also involved in the development and coloration of erythrophore in spotted scat [39]. Xanthine dehydrogenase (Xdh) and GTP cyclization hydrolase 1 (Gch1) were the key enzymes for the pteridine metabolic pathway [69]. In addition, *xdh* expression was significantly higher in red skin than that in gray skin of red crucian carp (*Carassius auratus*, red var.) [81]. In this study, the expressions of *xdh* and *gch1* were significantly up-regulated in red skins of spotted scat exposed to TU, suggesting the repression of thyroid hormone signaling in regulating pteridine metabolism. Taken together, thyroid hormone signaling may inhibit erythrophores formation and red coloration in spotted scat by affecting carotenoids and pteridine metabolism.

Most melanophores of the adult pattern, adult iridophores and some adult xanthophores develop from postembryonic neural crest–derived progenitors rather than directly from migrating neural crest cells [19, 82]. In zebrafish, larval melanophores differentiated sparsely, but could not migrate and began to die within the first week. Subsequently, a new *kita*-independent melanophores population was differentiated until a few weeks later, indicating the presence of latent cells with the potential for melanogenesis even in the post-embryonic stage. In spotted scat, larval melanophores and erythrophores gradually decreased and the trunk became transparent at 8 dpf. At the 14 dpf, a large number of erythrophores, iridophores, and melanophores was differentiated. Therefore, postembryonic progenitors may also exist in the postembryonic stage of spotted scat, and the adult chromatophores are derived from this population. Interactions between all three pigment cell types and their tissue environment are required for adult stripe development, iridophores normally prevent melanophores from accessing the interstripe region and simultaneously support stripe formation dorsally and ventrally [25]. In our results, thyroid hormone promotes the formation of iridophores, which may lead to the inhibition of melanophores and abnormal pigment pattern.

Conclusions

Spotted scat has variable body color patterns, including whole black, black bars, black and red spots. In this study, disruption of thyroid hormone signaling could stimulate the expression of genes associated with melanin synthesis pathway (*tyr*, *tyrp1*, *dct*, *oca2*, *mitf*, *pmel*, *slc24a5*, and *erbb3*), and the formation of adult melanophore and the black spots pattern. In contrast, thyroid hormone T3 could block the final body color patterns formation in spotted scat. More important, T3 could inhibit the development of larval erythrophores and reduce the accumulation of carotenoids. When blockage of thyroid hormone signaling with TU, the expression of genes involved in carotenoid (*apod*, *pnpla2*, *rdh12*, *stard10*, *abca1*, *retsat*, *scarb1*), and pteridine metabolism (*xdh*, *gch1*) was induced. In contrast, thyroid hormones act differently on iridophore than on the

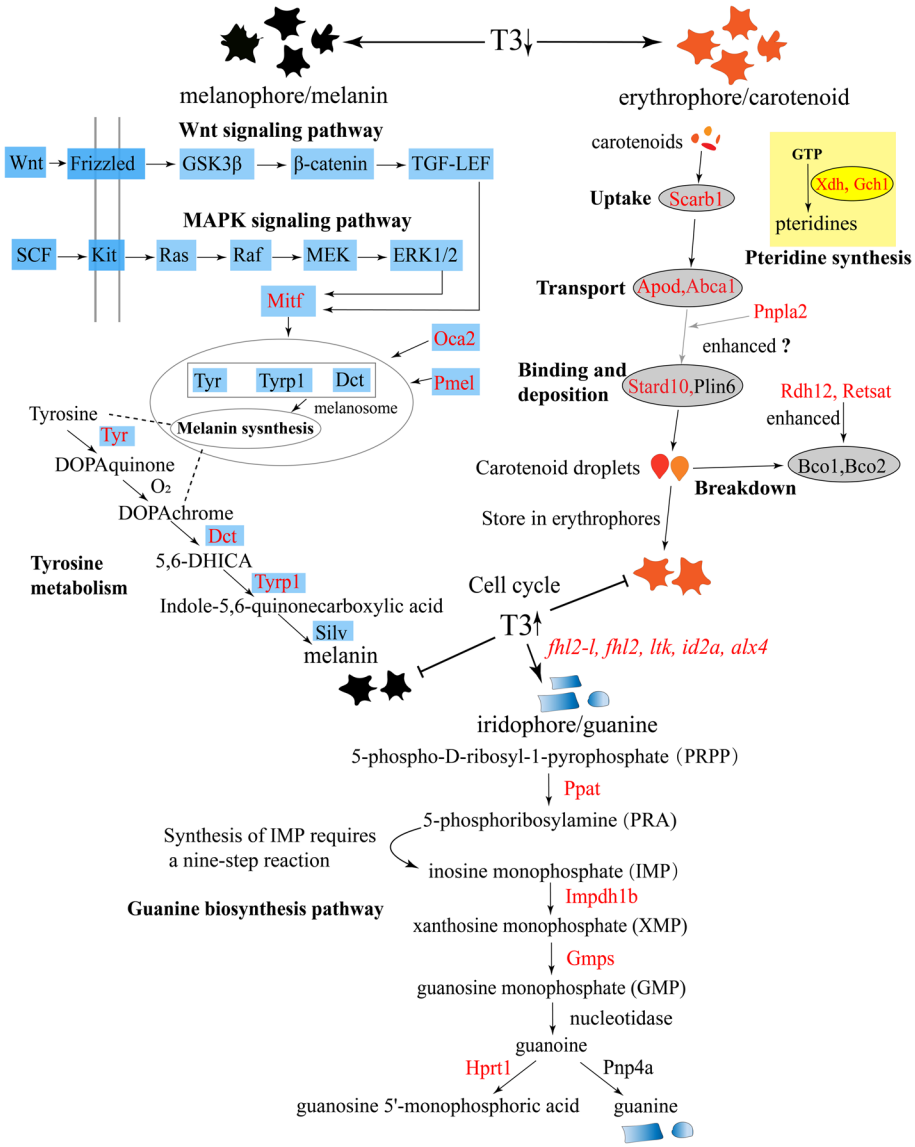

Fig. 8 Possible model between pigmentation gene expression and thyroid hormone signaling in spotted scat

other two types of cells. Thyroid hormone induces the expression of iridophore differentiation factors (*fhl2-l, fhl2, ltk, id2a, alx4*) and guanine synthesis genes (*gmps, hprt1, ppat, impdh1b*) and promotes iridophore formation (Fig. 8). This study could provide new insights for exploring the formation of body color patterns in fish, and help to elucidate the molecular mechanism of thyroid hormone in regulating in pigment cells development and body coloration.

Supplementary Information

The online version contains supplementary material available at https://doi.org/10.1186/s12864-025-11286-6.

Supplementary Material 1.

Acknowledgements
We thank Youxing Xie of Guangdong Ocean University (Zhanjiang, China) for providing us with the larval samples. We thank Bo Zhang of Development and Research Center for Biological Marine Resources, Southern Marine Science and Engineering Guangdong Laboratory (Zhanjiang, China) for his critique of this manuscript.

Authors' contributions
YGL carried out all the experiments, data analyses, and wrote the main text. TH extracted the RNA and revised the manuscript. DNJ revised the manuscript. GS and CHZ provided the experimental fish. GLL supervised the research. HJS supervised the research and revised the manuscript. All authors read and approved the final manuscript.

Funding
This research was supported by grants from the National Natural Science Foundation of China (grant numbers: 32002367 and 32201420), the Zhanjiang Science and Technology Plan Project (grant number: 2022A01046), the Guangdong Provincial Science and Technology Program (grant number: 2023B0202010005), Guangdong Basic and Applied Basic Research Foundation (grant number: 2023A1515012880 and 2024A1515010328), the Key Laboratory of Tropical Aquatic Germplasm of Hainan Province (Open Fund Project No. TAG-2024-KF-03).

Data availability
All clean libraries of RNA sequencing data have been submitted to the Sequence Read Archive (SRA) database (Accession No.: PRJNA1142162).

Declarations

Ethics approval and consent to participate
The experiment and animals were approved by the Institutional Animal Care and Use Committee (IA-CUS) of Guangdong Ocean University and complied with China's laws and regulations on biological research.

Competing interests
The authors declare no competing interests.

Author details
[1]Guangdong Research Center On Reproductive Control and Breeding Technology of Indigenous Valuable Fish Species, Guangdong Provincial Key Laboratory of Aquatic Animal Disease Control and Healthy Culture, Fisheries College, Guangdong Ocean University, Zhanjiang 524088, China. [2]Development and Research Center for Biological Marine Resources, Southern Marine Science and Engineering Guangdong Laboratory (Zhanjiang), Zhanjiang 524025, China.

Received: 11 October 2024 Accepted: 23 January 2025
Published online: 27 January 2025

References

1. Singh AP, Nüsslein-Volhard C. Zebrafish Stripes as a Model for Vertebrate Colour Pattern Formation. Curr Biol. 2015;25:R81-92.
2. Hendrick L, Carter G, Hilbrands E, Heubel B, Schilling T, Le Pabic P. Bar, stripe and spot development in sand-dwelling cichlids from Lake Malawi. EvoDevo. 2019;10.
3. Liang Y, Gerwin J, Meyer A, Kratochwil CF. Developmental and Cellular Basis of Vertical Bar Color Patterns in the East African Cichlid Fish *Haplochromis latifasciatus*. Front Cell Dev Biol. 2020;8:62.
4. Irion U, Singh AP, Nüsslein-Volhard C. The Developmental Genetics of Vertebrate Color Pattern Formation. In: Current Topics in Developmental Biology. Elsevier; 2016. p. 141–69.
5. Salis P, Lorin T, Laudet V, Frédérich B. Magic traits in magic fish: understanding color pattern evolution using reef fish. Trends Genet. 2019;35:265–78.
6. Schartl M, Larue L, Goda M, Bosenberg MW, Hashimoto H, Kelsh RN. What is a vertebrate pigment cell? Pigment Cell Melanoma Res. 2016;29:8–14.
7. Mort RL, Jackson IJ, Patton EE. The melanocyte lineage in development and disease. Development. 2015;142:1387.
8. Fang D, Tsuji Y, Setaluri V. Selective down-regulation of tyrosinase family gene *TYRP1* by inhibition of the activity of melanocyte transcription factor. MITF Nucleic Acids Res. 2002;30:3096–106.
9. Widlund HR, Fisher DE. Microphthalamia-associated transcription factor: a critical regulator of pigment cell development and survival. Oncogene. 2003;22:3035–41.
10. O'Gorman M, Thakur S, Imrie G, Moran RL, Choy S, Sifuentes-Romero I, et al. Pleiotropic function of the *oca2* gene underlies the evolution of sleep loss and albinism in cavefish. Curr Biol. 2021;31:3694-3701.e4.
11. Kratochwil CF, Urban S, Meyer A. Genome of the Malawi golden cichlid fish (*Melanochromis auratus*) reveals exon loss of *oca2* in an amelanistic morph. Pigment Cell Melanoma Res. 2019;32:719–23.
12. Klaassen H, Wang Y, Adamski K, Rohner N, Kowalko JE. CRISPR mutagenesis confirms the role of *oca2* in melanin pigmentation in *Astyanax mexicanus*. Dev Biol. 2018;441:313–8.
13. Hellström AR, Watt B, Fard SS, Tenza D, Mannström P, Narfström K, et al. Inactivation of Pmel Alters Melanosome Shape But Has Only a Subtle Effect on Visible Pigmentation. PLoS Genet. 2011;7:e1002285.
14. Huang D, Lewis VM, Foster TN, Toomey MB, Corbo JC, Parichy DM. Development and genetics of red coloration in the zebrafish relative *Danio albolineatus*. eLife. 2021;10.
15. Fang W, Huang J, Li S, Lu J. Identification of pigment genes (melanin, carotenoid and pteridine) associated with skin color variant in red tilapia using transcriptome analysis. Aquaculture. 2022;547: 737429.
16. Du J, Chen H, Mandal BK, Wang J, Shi Z, Lu G, et al. HDL receptor/Scavenger receptor B1-Scarb1 and Scarb1-like mediate the carotenoid-based red coloration in fish. Aquaculture. 2021;545: 737208.
17. Ma C. Teleost Metamorphosis: The Role of Thyroid Hormone. Frontiers in endocrinology. 2019;10.
18. McMenamin SK, Parichy DM. Chapter Five - Metamorphosis in Teleosts. In: Shi Y-B, editor. Current Topics in Developmental Biology. Academic Press; 2013. p. 127–65.
19. McMenamin SK, Bain EJ, McCann AE, Patterson LB, Eom DS, Waller ZP, et al. Thyroid hormone-dependent adult pigment cell lineage and pattern in zebrafish. Science. 2014;345:1358–61.
20. Laudet V. The origins and evolution of vertebrate metamorphosis. Curr Biol. 2011;21:R726-737.
21. Lema SC. Hormones, developmental plasticity, and adaptive evolution: Endocrine flexibility as a catalyst for "plasticity-first" phenotypic divergence. Mol Cell Endocrinol. 2020;502:110678.
22. Roux N, Miura S, Dussenne M, Tara Y, Lee S, De Bernard S, et al. The multilevel regulation of clownfish metamorphosis by thyroid hormones. Cell Rep. 2023;42:112661.
23. Holzer G, Besson M, Lambert A, François L, Barth P, Gillet B, et al. Fish larval recruitment to reefs is a thyroid hormone-mediated metamorphosis sensitive to the pesticide chlorpyrifos. Elife. 2017;6:e27595.
24. Huerlimann R, Roux N, Maeda K, Pilieva P, Miura S, Chen H-C, et al. The transcriptional landscape underlying larval development and metamorphosis in the Malabar grouper (*Epinephelus malabaricus*). Elife. 2024;13:RP94573.
25. Patterson LB, Parichy DM. Zebrafish Pigment Pattern Formation: Insights into the Development and Evolution of Adult Form. Annu Rev Genet. 2019;53:505–30.
26. Saunders LM, Mishra AK, Aman AJ, Lewis VM, Toomey MB, Packer JS, et al. Thyroid hormone regulates distinct paths to maturation in pigment cell lineages. Elife. 2019;8:e45181.
27. Hulbert AJ. Thyroid hormones and their effects: a new perspective. Biol Rev Camb Philos Soc. 2000;75:519–631.
28. Cheng S-Y, Leonard JL, Davis PJ. Molecular aspects of thyroid hormone actions. Endocr Rev. 2010;31:139–70.
29. Grøntved L, Waterfall JJ, Kim DW, Baek S, Sung M-H, Zhao L, et al. Transcriptional activation by the thyroid hormone receptor through ligand-dependent receptor recruitment and chromatin remodelling. Nat Commun. 2015;6:7048.
30. Rastorguev SM, Nedoluzhko AV, Levina MA, Prokhorchuk EB, Skryabin KG, Levin BA. Pleiotropic effect of thyroid hormones on gene expression in fish as exemplified from the blue bream *Ballerus ballerus* (Cyprinidae): Results of transcriptomic analysis. Dokl Biochem Biophys. 2016;467:124–7.
31. Guillot R, Muriach B, Rocha A, Rotllant J, Kelsh RN, Cerdá-Reverter JM. Thyroid Hormones Regulate Zebrafish Melanogenesis in a Gender-Specific Manner. PLoS ONE. 2016;11:e0166152.
32. Salis P, Roux N, Huang D, Marcionetti A, Mouginot P, Reynaud M, et al. Thyroid hormones regulate the formation and environmental plasticity of white bars in clownfishes. Proc Natl Acad Sci U S A. 2021;118:e2101634118.
33. Prazdnikov DV, Shkil FN. The role of thyroid hormones in the development of coloration of two species of Neotropical cichlids. J Exp Biol. 2023;226:jeb245710.
34. Prazdnikov DV. Thyroid hormone signaling in the evolution of pigment patterns in cichlids: results and research prospects. Hydrobiologia. 2024. https://doi.org/10.1007/s10750-024-05640-0.

35. Prazdnikov DV, Shkil FN. Experimental evidence of the role of heterochrony in evolution of the Mesoamerican cichlids pigment patterns. Evol Dev. 2019;21:3–15.
36. Prazdnikov D. Effect of Thyroid Hormones on the Development of Asymmetric Pigment Patterns in Teleost Fish: Experimental Data on the Example of *Amatitlania nigrofasciata* (Cichlidae) and *Poecilia wingei* (Poeciliidae). Biology Bulletin. 2020;47:198–204.
37. Dawes JHP, Kelsh RN. Cell Fate Decisions in the Neural Crest, from Pigment Cell to Neural Development. Int J Mol Sci. 2021;22:13531.
38. Lin X, Tian C, Huang Y, Shi H, Li G. Comparative Transcriptome Analysis Identifies Candidate Genes Related to Black-Spotted Pattern Formation in Spotted Scat (*Scatophagus argus*). Animals (Basel). 2021;11:765.
39. Liao Y, Shi H, Han T, Jiang D, Lu B, Shi G, et al. Pigment Identification and Gene Expression Analysis during Erythrophore Development in Spotted Scat (*Scatophagus argus*) Larvae. Int J Mol Sci. 2023;24:15356.
40. Karlsson J, von Hofsten J, Olsson P-E. Generating Transparent Zebrafish: A Refined Method to Improve Detection of Gene Expression During Embryonic Development. Mar Biotechnol. 2001;3:0522–7.
41. Korifi R, Le Dréau Y, Antinelli J-F, Valls R, Dupuy N. CIEL*a*b* color space predictive models for colorimetry devices–analysis of perfume quality. Talanta. 2013;104:58–66.
42. Zhang J, Tian C, Zhu K, Liu Y, Zhao C, Jiang M, et al. Effects of Natural and Synthetic Astaxanthin on Growth, Body Color, and Transcriptome and Metabolome Profiles in the Leopard Coralgrouper (*Plectropomus leopardus*). Animals (Basel). 2023;13:1252.
43. Clotfelter ED, Ardia DR, McGraw K. Red fish, blue fish: Trade-offs between pigmentation and immunity in Betta splendens. Behav Ecol. 2007;18:1139–45.
44. Grether GF, Hudon J, Endler JA. Carotenoid Scarcity, Synthetic Pteridine Pigments and the Evolution of Sexual Coloration in Guppies (*Poecilia reticulata*). Proceedings: Biological Sciences. 2001;268:1245–53.
45. Kim D, Langmead B, Salzberg SL. HISAT: a fast spliced aligner with low memory requirements. Nat Methods. 2015;12:357–60.
46. Florea L, Song L, Salzberg SL. Thousands of exon skipping events differentiate among splicing patterns in sixteen human tissues. F1000Res. 2013;2:188.
47. Love MI, Huber W, Anders S. Moderated estimation of fold change and dispersion for RNA-seq data with DESeq2. Genome Biol. 2014;15:550.
48. Young MD, Wakefield MJ, Smyth GK, Oshlack A. Gene ontology analysis for RNA-seq: accounting for selection bias. Genome Biol. 2010;11:R14.
49. Mao X, Cai T, Olyarchuk JG, Wei L. Automated genome annotation and pathway identification using the KEGG Orthology (KO) as a controlled vocabulary. Bioinformatics. 2005;21:3787–93.
50. Cuthill IC, Allen WL, Arbuckle K, Caspers B, Chaplin G, Hauber ME, et al. The biology of color. Science. 2017;357:eaan0221.
51. Balon EK. Epigenetic processes, when natura non facit saltum becomes a myth, and alternative ontogenies a mechanism of evolution. Environ Biol Fishes. 2002;65:1–35.
52. Parichy DM. Pigment patterns: fish in stripes and spots. Curr Biol. 2003;13:R947-950.
53. Patterson LB, Parichy DM. Interactions with iridophores and the tissue environment required for patterning melanophores and xanthophores during zebrafish adult pigment stripe formation. PLoS Genet. 2013;9:e1003561.
54. McGowan KA, Barsh GS. How the zebrafish got its stripes. eLife. 2016;5:e14239.
55. Irion U, Singh AP, Nüsslein-Volhard C. The developmental genetics of vertebrate color pattern formation: lessons from Zebrafish. Curr Top Dev Biol. 2016;117:141–69.
56. Kelsh RN, Harris ML, Colanesi S, Erickson CA. Stripes and belly-spots – a review of pigment cell morphogenesis in vertebrates. Semin Cell Dev Biol. 2009;20:90–104.
57. Yoo JH, Takeuchi T, Tagawa M, Seikai T. Effect of Thyroid Hormones on the Stage-specific Pigmentation of the Japanese Flounder *Paralichthys olivaceus*. Zoolog Sci. 2000;17:1101–6.
58. Braasch I, Liedtke D, Volff J-N, Schartl M. Pigmentary function and evolution of *tyrp1* gene duplicates in fish. Pigment Cell Melanoma Res. 2009;22:839–50.
59. Lu B, Liang G, Xu M, Wang C, Tan D, Tao W, et al. Production of all male amelanotic red tilapia by combining MAS-GMT and *tyrb* mutation. Aquaculture. 2022;546:737327.
60. Li H, Wang X, Zhang R, Liu L, Zhu H. Generation of golden goldfish *Carassius auratus* via tyrosinase gene targeting by CRISPR/Cas9. Aquaculture. 2024;583:740594.
61. Vogel P, Read RW, Vance RB, Platt KA, Troughton K, Rice DS. Ocular albinism and hypopigmentation defects in *Slc24a5*-/- mice. Vet Pathol. 2008;45:264–79.
62. Pandey D, Matsubara T, Saito T, Kazeto Y, Gen K, Sakuma T, et al. TALEN-Mediated Gene Editing of *slc24a5* (Solute Carrier Family 24, Member 5) in Kawakawa, *Euthynnus affinis*. J Marine Sci Eng. 2021. https://doi.org/10.3390/jmse9121378.
63. Gómez A, Volff J-N, Hornung U, Schartl M, Wellbrock C. Identification of a second egfr gene in Xiphophorus uncovers an expansion of the epidermal growth factor receptor family in fish. Mol Biol Evol. 2004;21:266–75.
64. Baldini E, Odorisio T, Tuccilli C, Persechino S, Sorrenti S, Catania A, et al. Thyroid diseases and skin autoimmunity. Rev Endocr Metab Disord. 2018;19:311–23.
65. Ma H, Yang F, Ding X-Q. Deficiency of thyroid hormone receptor protects retinal pigment epithelium and photoreceptors from cell death in a mouse model of age-related macular degeneration. Cell Death Dis. 2022;13:255.
66. Tanizaki Y, Shibata Y, Zhang H, Shi Y-B. Analysis of thyroid hormone receptor α-knockout tadpoles reveals that the activation of cell cycle program is involved in thyroid hormone-induced larval epithelial cell death and adult intestinal stem cell development during *Xenopus tropicalis* metamorphosis. Thyroid. 2021;31:128–42.
67. Tanizaki Y, Zhang H, Shibata Y, Shi Y-B. Thyroid hormone receptor α controls larval intestinal epithelial cell death by regulating the CDK1 pathway. Commun Biol. 2022;5:112.
68. Hoekstra HE. Genetics, development and evolution of adaptive pigmentation in vertebrates. Heredity (Edinb). 2006;97:222–34.
69. Ziegler I, McDonald T, Hesslinger C, Pelletier I, Boyle P. Development of the pteridine pathway in the zebrafish. Danio rerio J Biol Chem. 2000;275:18926–32.
70. Prazdnikov DV, Shkil FN. Effects of hyperthyroidism on the Labeobarbus (= Barbus) intermedius (Cyprinidae) early larval melanophores development. J Ichthyol. 2016;56:321–4.
71. Salis P, Lorin T, Lewis V, Rey C, Marcionetti A, Escande M-L, et al. Developmental and comparative transcriptomic identification of iridophore contribution to white barring in clownfish. Pigment Cell Melanoma Res. 2019;32:391–402.
72. Lewis VM, Saunders LM, Larson TA, Bain EJ, Sturiale SL, Gur D, et al. Fate plasticity and reprogramming in genetically distinct populations of *Danio* leucophores. Proc Natl Acad Sci. 2019;116:11806–11.
73. Cal L, Suarez-Bregua P, Cerdá-Reverter JM, Braasch I, Rotllant J. Fish pigmentation and the melanocortin system. Comp Biochem Physiol A: Mol Integr Physiol. 2017;211:26–33.
74. Luo M, Lu G, Yin H, Wang L, Atuganile M, Dong Z. Fish pigmentation and coloration: Molecular mechanisms and aquaculture perspectives. Rev Aquac. 2021;13:2395–412.
75. Reboul E, Borel P. Proteins involved in uptake, intracellular transport and basolateral secretion of fat-soluble vitamins and carotenoids by mammalian enterocytes. Prog Lipid Res. 2011;50:388–402.
76. Walsh N, Dale J, McGraw KJ, Pointer MA, Mundy NI. Candidate genes for carotenoid coloration in vertebrates and their expression profiles in the carotenoid-containing plumage and bill of a wild bird. Proc Biol Sci. 2012;279:58–66.
77. Eriksson J, Larson G, Gunnarsson U, Bed'hom B, Tixier-Boichard M, Strömstedt L, et al. Identification of the yellow skin gene reveals a hybrid origin of the domestic chicken. PLoS Genet. 2008;4:e1000010.
78. Gao G-Q, Song L-S, Tong B, Li G-P. Expression levels of *GSTA2* and *APOD* genes might be associated with carotenoid coloration in golden pheasant (*Chrysolophus pictus*) plumage. Dongwuxue Yanjiu. 2016;37:144–50.
79. Toomey MB, Lind O, Frederiksen R, Curley RW, Riedl KM, Wilby D, et al. Complementary shifts in photoreceptor spectral tuning unlock the full adaptive potential of ultraviolet vision in birds. Elife. 2016;5:e15675.

80. Ahi EP, Lecaudey LA, Ziegelbecker A, Steiner O, Glabonjat R, Goessler W, et al. Comparative transcriptomics reveals candidate carotenoid color genes in an East African cichlid fish. BMC Genomics. 2020;21:54.
81. Zhang Y, Liu J, Peng L, Ren L, Zhang H, Zou L, et al. Comparative transcriptome analysis of molecular mechanism underlying gray-to-red body color formation in red crucian carp (*Carassius auratus, red var.*). Fish Physiol Biochem. 2017;43:1387–98.
82. Singh AP, Schach U, Nüsslein-Volhard C. Proliferation, dispersal and patterned aggregation of iridophores in the skin prefigure striped colouration of zebrafish. Nat Cell Biol. 2014;16:604–11.

Publisher's Note